The Journal of Veterinary Medical Science

FULL PAPER

Immunology

Flow cytometric analysis of bronchoalveolar lavage fluid immune dynamics in calves

Shingo ISHIKAWA[1)], Masataka MIYAZAWA[2)], Yoshinori ZIBIKI[2)], Rie KAMIKAKIMOTO[2)] and Seiji HOBO[2)]*

[1)]Division of Veterinary Science, Graduate School of Life and Environmental Biosciences, Osaka Prefecture University, Osaka, Japan
[2)]Joint Faculty of Veterinary Medicine, Kagoshima University, Kagoshima, Japan

ABSTRACT. Understanding the immune dynamics in the respiratory mucosa of calves is necessary for a good management of bovine respiratory disease. Immune dynamics in the respiratory mucosa in humans and experimental animals has been assessed by flow cytometric analysis of bronchoalveolar lavage fluid (BALF); however, few reports have addressed this subject in calves. The aim of this study was to establish a universal method to analyze bronchoalveolar lavage fluid (BALF) by flow cytometry and to obtain basic knowledge of bovine respiratory mucosal immune dynamics. We investigated the immune cell populations in BALF and evaluated the surface antigen expression of alveolar macrophages in calves using flow cytometer. To further analyze the surface antigen variation observed in alveolar macrophages in detail, stimulation assays were performed *in vitro*. BALF cells were separated into three distinct populations based on their light scatter plot, which were considered to be macrophages, lymphocytes, and neutrophils. In most individuals, most of the BALF immune cells were alveolar macrophages, but an increased proportion of lymphocytes and neutrophils was observed in some individuals. Analysis of each surface antigen expression in alveolar macrophages showed that CD21 and MHC class II expression changed in response to changes in the leukocyte population. Moreover, when alveolar macrophages were stimulated with interferon-γ *in vitro*, the expression of CD21 was drastically reduced and MHC class II was increased, suggesting that functional changes in alveolar macrophages themselves are involved in the immune dynamics.

KEYWORDS: alveolar macrophage, bronchoalveolar lavage, calf, flow cytometry, mucosal immunology

J. Vet. Med. Sci.
84(4): 548–557, 2022
doi: 10.1292/jvms.21-0522

Received: 28 September 2021
Accepted: 30 January 2022
Advanced Epub:
10 February 2022

Bovine respiratory disease (BRD) is one of the most common and expensive to treat diseases in domesticated animals [12], and hence, reducing its incidence will have a great economic impact [16]. In the neonatal to infantile period, the immune system is still immature and susceptibility to BRD is high [8]. Although immune dynamics in the respiratory mucosa in humans and experimental animals has been elucidated by flow cytometric analysis of bronchoalveolar lavage fluid (BALF) [13], little is known about the same in cattle. The lack of knowledge about respiratory mucosal immune dynamics in cattle is said to be hindering the development of effective vaccine [21].

Flow cytometry is the gold standard for analyzing immune dynamics, but it has several limitations. Until about a decade ago, compared to findings in experimental animals, human respiratory mucosal immune dynamics have not been analyzed in detail owing to high autofluorescence of alveolar macrophages [2, 24]. Recent innovations in flow cytometers and fluorescent dyes have led to the development of detailed analytical methods [25] that have greatly contributed to the understanding of pathogenesis of respiratory diseases [11]. Development of a flow cytometric method to analyze bovine respiratory mucosal dynamics may help improved our understanding of BRD pathogenesis. In addition, the complexity and sensitivity of flow cytometric analysis have highlighted the importance of standardizing sample analysis [10]. Therefore, it is important to develop a method that is as convenient and high-throughput as possible. Nonetheless, to our knowledge, no studies have reported such standardized methods for cattle.

Alveolar macrophages are the most important and abundant immune cells that provide a defense mechanism in the lungs because they are responsible for phagocytosis of pathogens [4]. Studies in experimental animals have shown that alveolar macrophages have plasticity, and they control infection and inflammation in the respiratory tract by changing their phenotype and

*Correspondence to: Hobo, S.: k2088185@kadai.jp, Joint Faculty of Veterinary Medicine, Kagoshima University, 1-21-24 Korimoto, Kagoshima 890-0065, Japan

function depending on infectious agents and inflammatory conditions [14]. In particular, interferon gamma (IFN-γ) is known to be strongly involved in the functional changes of alveolar macrophages [2]. It is assumed that bovine alveolar macrophage function is also affected in response to dynamic changes in respiratory mucosa. Several reports have focused on the direct crosstalk between pathogens and bovine alveolar macrophages [1, 3]; nevertheless, to our knowledge, variations from basic steady-state bovine alveolar macrophage characteristics and their relationship to other immune cell populations have not been addressed.

The aim of this study was to establish a universal method to analyze bronchoalveolar lavage fluid (BALF) by flow cytometry and to obtain basic knowledge of bovine respiratory mucosal immune dynamics especially alveolar macrophages. In experiment 1, we evaluated the technique of flow cytometry to investigate immune cell dynamics in BALF and phenotypic markers of alveolar macrophages of neonatal and infantile calves. In experiment 2, we have shown that cytokine IFN-γ drastically alters surface antigen expression at the gene expression level of bovine alveolar macrophages.

MATERIALS AND METHODS

Experiment 1

Animals: Six unrelated Holstein male calves were used in this study. All animals were cared for in accordance with the Guide for the Care and Use of Laboratory Animals of the Joint Faculty of Veterinary Medicine, Kagoshima University. Sampling was done twice from the same individual, in neonates (NE; 15–19-days old) and infants (IN; 41–48-days old). All animals were systemically healthy, and none had a chronic or immediate history of respiratory disease.

BALF processing: BALF was collected from the right cranial lobe using a flexible electronic endoscope (VQ TYPE 5112B; Olympus, Tokyo, Japan). The flexible electronic endoscope was inserted into a subsegment of each lobe. Three 30-ml aliquots of sterile 0.9% normal saline solution were instilled into the lobe and immediately aspirated. All aspiration was pooled and the volume of BALF was measured and recorded. BALF was immediately placed on ice and processed within 3 hr of collection. Some of the BALF was used for microbiological testing and confirmed to be negative for microbial pathogens. BALF was filtered through a cotton gauze and centrifuged at 400 × *g* for 10 min. The supernatant was removed by aspiration and the cell pellet was resuspended in 10 ml of phosphate-buffered saline (PBS) and counted using a cell counter (Countess; Invitrogen, Eugene, OR, USA).

Flow cytometric analysis: The BALF cells were resuspended in fluorescence activated cell sorting (FACS) buffer (PBS containing 0.5% BSA, pH 7.2) at 5 × 10^5 cells/100 µl. The cells were incubated with antibodies reactive with the following molecules: CD3 (Washington State University and VMRD, Pullman, WA, USA, Clone MM1A), CD11b (WSU; MM12A), CD11c (WSU; clone BAQ153A), CD14 (WSU; clone CAM66A), CD21 (WSU; clone GB25A), CD172a (WSU; clone DH59B), major histocompatibility complex (MHC) class II (WSU; clone BOV-CAT82A), neutrophils (WSU; clone CH138A) at 4°C for 30 min. All antibodies were diluted at 1:100. The cells were washed twice with the FACS buffer and resuspended in 100 µl of the FACS buffer. The cells that were incubated with CD3, CD11b, CD21, CD172a, and MHC Class II were incubated with anti-mouse IgG1 secondary antibodies labeled with phycoerythrin (PE) (diluted 1:1,000: Biolegend, San Diego, CA, USA), and CD11c, CD14, and the neutrophils were incubated with anti-mouse IgM secondary antibodies labeled with fluorescein isothiocyanate (FITC) (diluted 1:1,000: Biolegend, San Diego, CA, USA) at 4°C for 30 min. Nonspecific anti-mouse IgG1 labeled with PE (Biolegend; clone MG1-45) and anti-mouse IgM labeled with FITC (Biolegend; clone MM-30) were used as negative controls. Cells were then washed twice with the FACS buffer. After washing, the cells were stained using 7-aminoactinomycin D (7-AAD; Immunostep, Salamanca, Spain), which binds to deoxyribonucleic acid (DNA) when cell membrane permeability is altered after cell death, in accordance with the manufacturer's protocol. Cell suspensions were analyzed using BD Accuri™ C6 Plus flow cytometer (BD Biosciences, Franklin Lakes, NJ, USA), and the results were analyzed using FlowLogic software (Inivai Technologies, Mentone, Australia). Data were collected for the entire population of cells.

Cytological examination: Cytospins were prepared using cells obtained from the same BALF samples as those used for flow cytometry. The cells resuspended in PBS containing 0.5% BSA at 5 × 10^4 cells/100 µl were centrifuged onto a microscope slide using Thermo Shandon Cytospin 4 (Thermo Fisher Scientific Inc.; Waltham, MA, USA), at 500 rpm for 5 min at room temperature. The slides were air-dried, stained with Diff-Quick solution (Sysmex, Kobe, Japan), and counted under the light microscope. Two hundred cells were counted per cytospin and the differential cell count was morphologically determined.

Phagocytosis assay: Processed BALF cells (5 × 10^5 cells) were centrifuged at 500 × *g* for 3 min and resuspended in 1 ml of pHrodo™ Green *E. coli* BioParticles™ (Invitrogen) as per the manufacturer's instruction. Cells were seeded in two 24-well plates (500 µl) and were incubated at 4°C and 37°C in humidified 5% CO_2. Subsequently, the bioparticle-containing medium was removed and the cells were washed with PBS, and then, harvested by incubation with 1 mM ethylenediaminetetraacetic acid/PBS. The harvested cells were centrifuged at 500 × *g* for 3 min and resuspended in 500 µl of FACS buffer for analysis through flow cytometry. The occurrence of phagocytosis was identified by pHrodo green positive cells (pHrodo green fluorescence was measured using 533/30 nm filter: FL1). The temperature condition of 4°C was used as the negative control.

Experiment 2

Animals: Four unrelated age-matched, 52–60-days old Holstein male calves that were different from those used in Experiment 1 were used in this study. The feeding environment and the conditions of the animals were the same as those in Experiment 1.

BALF processing and flow cytometric analysis: BALF processing was performed using the same method as that in Experiment 1. Flow cytometric analysis was also performed as described in Experiment 1 but measurements were performed using FACSCalibur™ flow cytometer (BD Biosciences). The FACSCalibur™ and BD Accuri™ C6 Plus flow cytometers have the same

laser and filter configuration, and hence, the results of the analysis were not affected and were comparable (data not shown).

IFN-γ stimulation of alveolar macrophage culture: Isolated BALF cells were layered in 20 ml of sample over two 4-ml Lympholyte-H (Cederlane Lab., Ontario, Canada) in a 15-ml tube. The suspension was centrifuged for 60 min at 800 × *g* at room temperature. The interface layer was placed into a new 15-ml tube and washed three times with PBS. After an additional wash, the cells were resuspended in the complete medium [CM; RPMI-1640 medium (Wako Pure Chemical Industries, Osaka, Japan), 10% fetal bovine serum (Japan Bioserum, Hiroshima, Japan), 1% penicillin–streptomycin–amphotericin B solution (Wako Pure Chemical Industries) at 5×10^5 cells/ml. The cells were seeded in a 6-well plate (5 ml) and a 24-well plate (1 ml) and were incubated at 37°C in humidified 5% CO_2. After 12 hr, the non-adherent cells were removed and the CM was replaced, followed by stimulation with 5 ng/ml bovine recombinant IFN-γ (Invitrogen) for 72 hr. The preliminary study was performed at 24 hr, 48 hr, and 72 hr of culture, and the largest response was at 72 hr (data not shown).

Quantitative real-time reverse transcription PCR (RT q-PCR): The cells were harvested with 1 ml of RNAiso Plus reagent (Takara, Kusatsu, Japan) and the RNA was isolated using Direct-zol RNA MiniPrep Kit in accordance with the manufacturer's protocol (Zymo Research Corp., Irvine, CA, USA). The total cDNA was generated from 1 µg of the total RNA using a PrimeScript RT Reagent Kit with gDNA Eraser, as described by the manufacturer (Takara). RT q-PCR reactions were carried out with Perfect Real Time SYBR Premix Ex Taq II (Takara) using a StepOnePlus™ Real-Time PCR System (Applied Biosystems, Foster City, CA, USA) and the following shuttle PCR protocol: 95°C for 30 sec, followed by 40 cycles at 95°C for 5 sec and 60°C for 30 sec in a 20-µl reaction volume containing 2 µl of template cDNA, 0.8 µl of primers (0.4 µl of each), 10 µl of SYBR Premix Ex Taq II, 0.4 µl of ROX Reference Dye, and 6.0 µl of distilled water. Gene-specific primers are listed in Table 1. Changes in gene expression were calculated using the ΔΔC (T) method. All experiments were independently replicated twice.

Statistical analysis: Statistical analysis was conducted using commercially available statistical software (Prism 7.0; GraphPad Software, San Diego CA, USA). Paired *t*-tests were performed to analyze the differences between groups in each assay. The Pearson product moment correlation coefficient was used to calculate correlations. A P-value <0.05 was considered to reflect a statistically significant difference.

RESULTS

Experiment 1

Flow cytometric analysis of immune cells in the BALF: The cells in the BALF were analyzed using forward scatter-area (FSC-A) versus side scatter-area (SSC-A); however, it was difficult to separate them into distinct cell populations owing to the influence of debris and dead cells (Fig. 1A). Debris and dead cells were removed by backgating (Fig. 1B), and FSC-A versus SSC-A analysis was performed to classify cells into three distinct subpopulations. The subpopulation R1, located to the right in the contour plot, represented larger cells. The mean values of autofluorescence median fluorescence intensity (MFI) of FL1 and FL2 were 4,296 and 1,998, respectively, and these strongly expressed the macrophage marker CD172a (Fig. 1D). The subpopulation R2, aggregated to the lower left in the contour plot, corresponding to the lymphocyte population in peripheral blood. The mean values of autofluorescence MFI of FL1 and FL2 were 332 and 160, respectively, and an average of 67% of the cells expressed CD3, which is the T lymphocyte marker (Fig. 1E). The R3 subpopulation, located in the middle of the contour plot, corresponded to the neutrophil population in peripheral blood. The autofluorescence of FL1 and FL2 in the R3 region showed high (R3-H) and low (R3-L) populations (Fig. 1F). Even during backgating for R3-H and R3-L, they were mixed in the R3 region on the FSC-A versus SSC-A plot (data not shown), and hence, were difficult to separate. Therefore, it was difficult to analyze the clear positivity of R3-H in PE and FITC staining because the positive cells of R3-L overlapped with the isotype staining of R3-H. The diagonal-gating method described below could not be applied because of the presence of two cell populations. For R3-L, the histogram was completely separated from the isotype staining, suggesting that it strongly expressed the neutrophil marker.

As a result of morphological differential cell counts by cytospin, almost all the immune cell ratios present in BALF were macrophages in the NE (Table 2). Lymphocytes and neutrophils were found in the IN, and their proportions varied widely among individuals. Comparing the results of the differential cell counting method by cytospin and flow cytometry, the two methods correlated very well. For each identified cell type, Pearson correlation coefficients were calculated. For macrophages versus

Table 1. Sequences of primers used for PCR

Primer	Kind	Sequence (5′-3′)	Position	Accession number
GAPDH	Sense	GGCGTGAACCACGAGAAGTATAA	466–497	NM_001034034.1
	Antisense	CCCTCCACGATGCCAAAGT	566–584	
CD21	Sense	GCTGGAGCCTGGAAGAATGT	4,177–4,196	NM_001198991.1
	Antisense	AGGAGCAAGTGAACTGGGTG	4,196–4,177	
BoLA-DRB3	Sense	GAATGGAGGGCACGGTCTGA	697–716	NM_001012680.2
	Antisense	CCTTTCCATGCTGTGAAGAAGC	893–914	
BoLA-DRA	Sense	TGCCCACAACAGAGGATGTC	616–635	NM_001012677.1
	Antisense	GGAGCTTCATACTCCCAGTGC	683–703	
CIITA	Sense	AGAGAACTGAGCCTCCCACA	3,481–3,500	XM_585540.8
	Antisense	CACCACAATACCACGTCCCA	3,581–3,600	

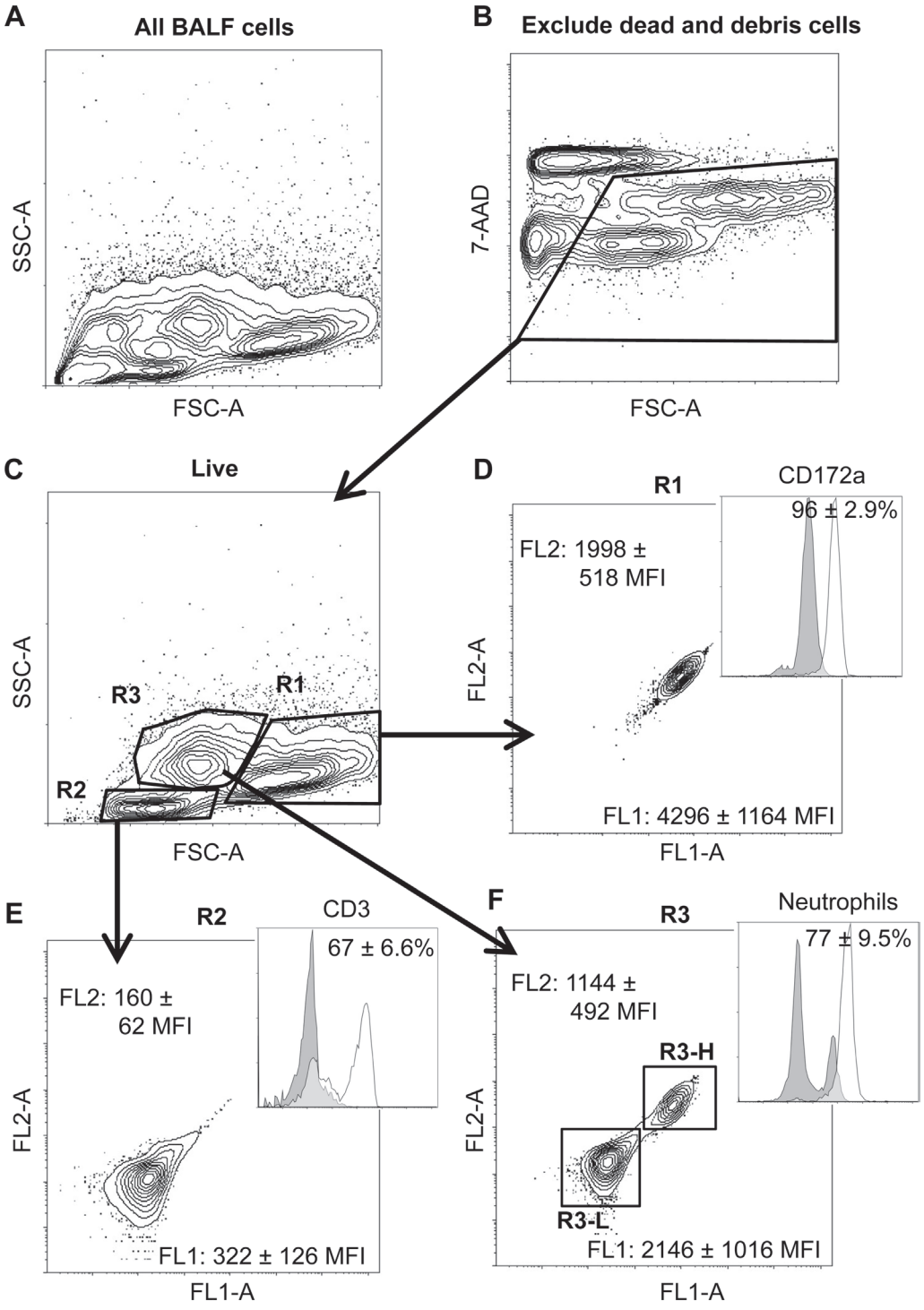

Fig. 1. Gating strategies for immune cells in bronchoalveolar lavage fluid (BALF). (**A**) Total cellular events in BALF were viewed in forward scatter-area (FSC-A) versus side scatter-area (SSC-A) flow cytometry dot plots. (**B**) Dead cells and debris were removed by 7-AAD staining and FSC-A gating. (**C**) From the FSC-A versus SSC-A contour plot, three cell populations, R1, R2, and R3, were gated. (**D**–**F**) Unstained R1, R2, and R3 subpopulations were analyzed in a contour plot of fluorescence 1 (FL1) and fluorescence 2 (FL2). The mean ± standard deviation (SD) of median fluorescence intensity of autofluorescence (MFI) are described. Overlaid histograms and positive cell mean ± SD stained with CD172a for R1 region, CD3 for R2 region, and neutrophils for R3 region are shown in the upper right section. Solid histograms show isotype control staining and open histograms show specific staining of the indicated marker. The R3 region was gated by two cell populations, R3-L and R3-H, in the FL1 versus FL2 plot.

R1 (r=0.94), lymphocytes versus R2 (r=0.97), and neutrophils versus R3 (r=0.97), the correlation coefficient was statistically significant (P<0.0001). Based on these results, R1 was defined as the alveolar macrophage region, R2 as the lymphocyte region, and R3 as the neutrophil region.

Table 2. Differential cell counts of bronchoalveolar lavage fluid

	No.	Percent cells by Cytospins						Percent cells by Flowcytometry					
		Macrophages		Lymphocytes		Neutrophils		R1		R2		R3	
		Neonatal	Infantile	Neonatal	Infantile	Neonatal	Infantile	Neonatal	Infantile	Neonatal	Infantile	Neonatal	Infantile
	1	99	82	0.5	9	0.5	9	91	83	0.75	6.7	0.77	5.0
	2	100	87	0.0	5.5	0.0	8	85	85	0.95	3.8	0.92	5.4
	3	100	59	0.0	15	0.5	26	80	45	1.83	14	3.8	27
	4	99	54	0.5	17	1.0	29	86	43	1.20	20	1.7	27
	5	99	56	0.5	9	0.5	41	83	29	0.53	7.7	0.68	49
	6	100	56	0.0	14	0.0	42	82	35	0.32	15	0.44	34
Average		99	66	0	12	0	26	85	53	0.9	11	1.4	24
SD		0.6	15	0.3	4.4	0.4	15	3.8	25	0.5	6.2	1.3	17
t-test *P*-value		**0.002		**0.001		**0.008		*0.019		**0.009		*0.021	
		Macrophages vs. R1		Lymphocytes vs. R2		Neutrophils vs. R3							
Pearson r		0.94		0.97		0.97							
P value		<0.0001		<0.0001		<0.0001							

*: $P<0.05$, **: $P<0.01$.

Surface antigen expression on alveolar macrophages: Based on the above-mentioned results, leukocyte populations in BALF were classified into three dynamics: NE (Fig. 2A), IN comprising almost exclusively macrophages (IN1: Fig. 2B), and IN comprising distinct neutrophils and lymphocytes (IN2: Fig. 2C). Analysis of the expression of each surface antigen showed that CD11c and CD14 were lowly expressed, whereas CD172a was highly expressed in all three populations. For CD11b, CD21, and MHC class II expression, showed a bimodal response that depended on the leukocyte population. Thus, it is suggested that their expression of alveolar macrophages was plastic and adapts to the alveoli microenvironment. Noteworthy, the expression of CD21 was significantly increased by more than 2-fold during the infantile period compared with that during the neonatal period (Table 3: $P=0.009$).

Changes in characteristics of alveolar macrophage: Fluorescence intensity was compared with isotype controls to estimate the percentage of cells positive for each antibody among alveolar macrophages. Alveolar macrophages have strong autofluorescence, and when the percentage of positive cells was analyzed using the histogram, the values were low due to the overlap (Fig. 3A-i). As shown in Fig. 3A-ii and Fig. 3A-iii, we were able to analyze the percentage of target positive cells without overlap by developing a contour plot with FL3-A and diagonal gating. Bimodal histograms of CD11b, CD21, and MHC class II expression rates were compared between the NE and IN, and the expression of CD21 was significantly increased in the infantile ($P=0.0007$) (Fig. 3B). MFI also increased indicating that both the expression rate and the expression level of CD21 increased from NE to IN.

The percentage of fluorescing cells after co-culture of pHrodo and alveolar macrophages at 37°C for 1 hr was analyzed using flow cytometry in comparison with cells co-cultured at 4°C for 1 hr (Fig. 3C). The used bioparticles emit fluorescence only after the particles were digested by the cell, and phagocytic ability could be analyzed. Phagocytic ability was significantly increased in IN compared to NE ($P=0.0014$).

To investigate the factors that cause variation in the MHC class II expression, the percentage of cells expressing MHC Class II and the percentage of cells in the R2 (lymphocyte) region were analyzed using Pearson's correlation coefficient (Fig. 3D) and showed a significant positive correlation (r=0.72, $P=0.009$).

Experiment 2

Effect of IFN-γ on alveolar macrophages: We analyzed the cell surface antigen and mRNA expression after *in vitro* stimulation with IFN-γ in alveolar macrophages. Stimulation of alveolar macrophages with IFN-γ led to a significant and drastic downregulation of CD21 expression ($P=0.022$) and upregulation of MHC class II expression ($P=0.019$) when compared to that in CM culture (Fig. 4A).

To evaluate the changes in surface antigen expression induced by IFN-γ, the mRNA expression of CD21 and MHC class II-related genes were analyzed by RT-qPCR (Fig. 4B). IFN-γ stimulation decreased CD21 mRNA expression by less than 2–3-fold, whereas MHC class II-related genes (encoding MHC class II molecules)—BoLA-DRB3 and BoLA-DRA—were increased by more than 2-fold and the class II major histocompatibility complex transactivator (CIITA), a regulator of MHC class II genes, was by more than 2–3-fold.

DISCUSSION

We report a method for analyzing immune cells in BALF of calves using a convenient and simple two-laser flow cytometer. The distribution of leukocyte counts in peripheral blood has a clear localization based on size and complexity and can be easily gated by FSC vs. SSC plots, whereas BALF cells show a dispersed population, which has been difficult to gate [23]. In this study, we succeeded in separating BALF cells into three distinct cell populations by backgating after the removal of debris and dead cells.

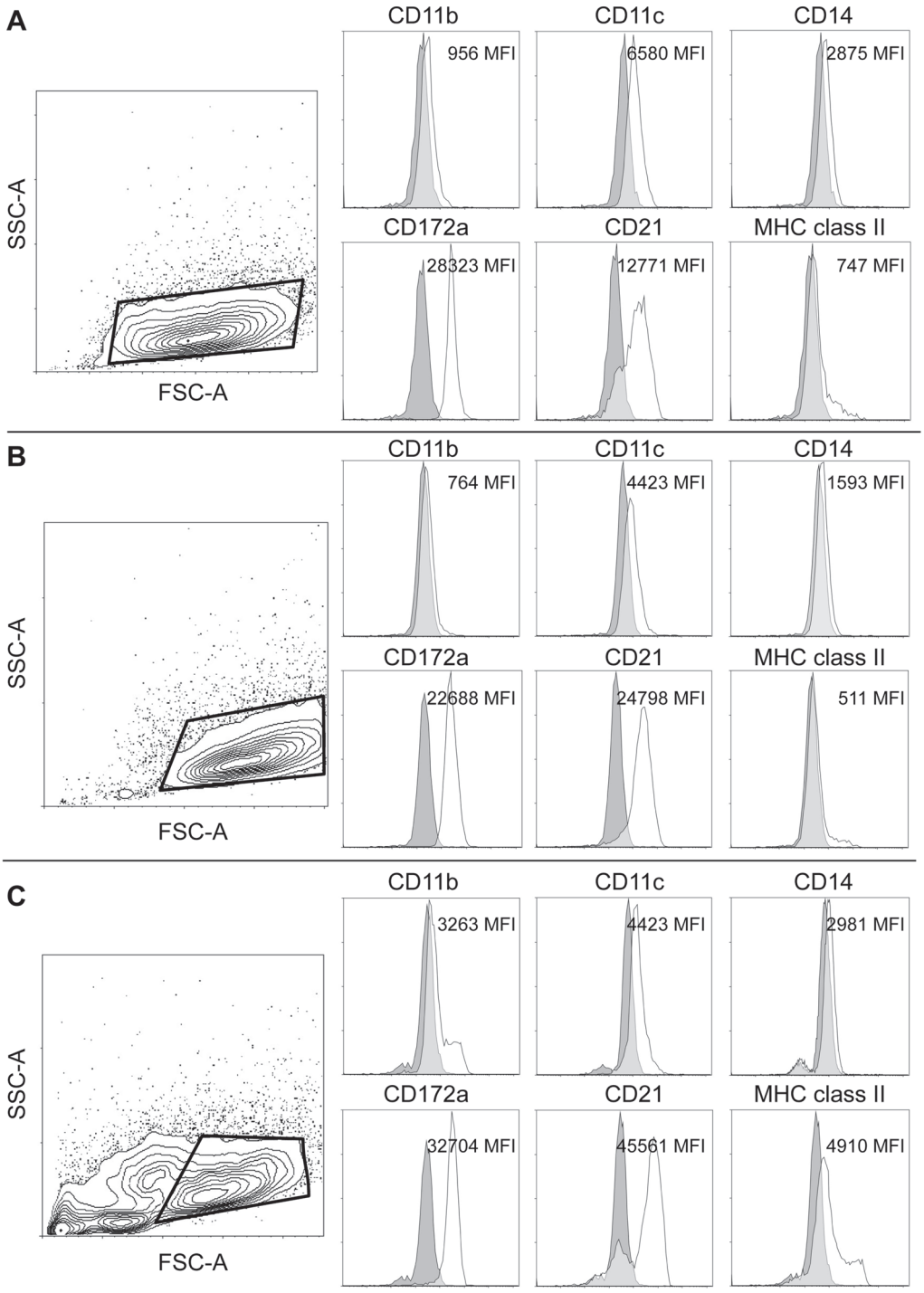

Fig. 2. Representative staining of alveolar macrophages. Surface antigen expression of alveolar macrophages in neonates (**A**), infants almost exclusively with macrophages (**B**), and infants with distinct neutrophils and lymphocytes (**C**) are shown in BALF. Solid histograms show isotype control staining and open histograms show specific staining of the indicated marker. Median fluorescent intensity (MFI) values were calculated by subtracting isotype control antibody staining from each antibody staining.

Based on the correlation with morphological differential cell counts using cytospin and the results of surface antigen expression analysis, the three cell populations were confirmed as macrophages, lymphocytes, and neutrophils. Reports have defined cytometric panels for BALF with similar light scattering profiles in humans [7, 10].

In the neutrophilic region, two populations with different autofluorescence were identified. The autofluorescence of neutrophils in BALF was more than doubled by bacterial infection in humans and mice [20]. Two populations of neutrophils with autofluorescence may be cells that have been stimulated or unstimulated in some way.

Table 3. Median Fluorescence intensity (MFI) of alveolar macrophage surface marker

	No.	MFI of CD11b		MFI of CD11c		MFI of CD14		MFI of CD172a		MFI of CD21		MFI of MHC Class II	
		Neonatal	Infantile	Neonatal	Infantile	Neonatal	Infantile	Neonatal	Infantile	Neonatal	Infantile	Neonatal	Infantile
	1	956	764	6,580	4,423	2,875	1,593	28,323	22,688	12,771	24,798	747	511
	2	1,741	1,125	10,867	7,679	2,379	1,873	30,810	22,024	6,375	21,483	570	396
	3	652	896	3,908	4,545	2,408	2,424	26,985	32,979	12,161	24,634	507	1,301
	4	1,968	942	11,965	3,995	2,211	1,956	23,402	44,620	8,381	41,829	692	1,285
	5	3,746	4,322	7,657	8,156	5,275	2,124	26,193	28,674	1,574	20,060	436	1,425
	6	550	3,263	3,398	8,560	3,679	2,981	19,867	32,705	12,061	45,561	371	4,910
Average		1,602	1,885	7,396	6,226	3,138	1,402	25,930	30,615	8,887	29,727	554	1,638
SD		1,198	1,519	7,532	6,527	1,175	907	3,844	8,325	4,380	11,034	146	1,662
t-test *P*-value		0.52		0.20		0.20		0.59		**0.009		0.19	

MFI values were calculated by subtracting isotype control antibody staining from each antibody staining. **: $P<0.01$.

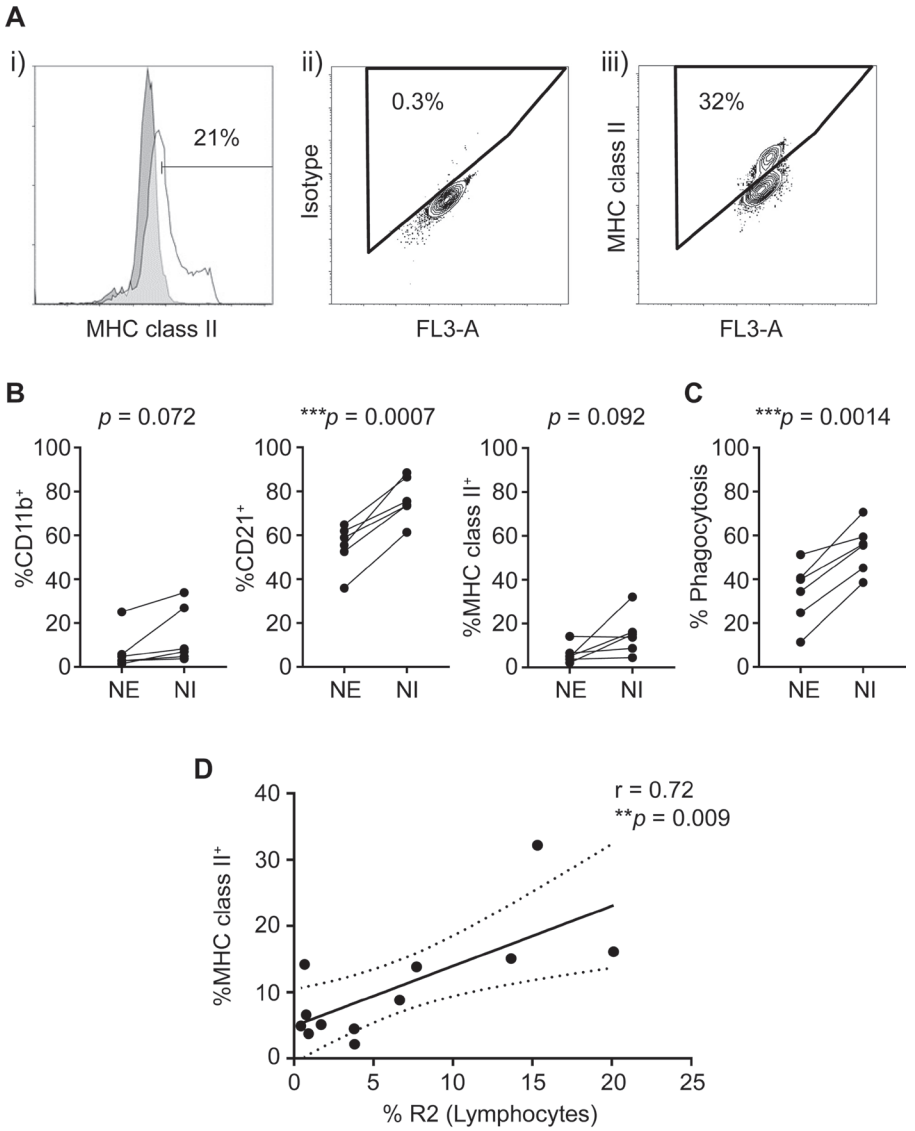

Fig. 3. (**A**) Strategies for estimating the percentage of cells positive for each antibody among alveolar macrophages. Histogram analysis showed that the percentage of MHC class II expression was 21% (i), but the percentage increased to 32% when a contour plot was developed with FL3-A and diagonal gating (ii and iii). (**B**) The percentages of CD11b, CD21, and MHC class II were positivity calculated by contour plot analysis and compared between neonates (NE) and infants (IN). The figures (circles) of the same individual are connected by lines. (**C**) The results of phagocytosis assays measured by co-culturing alveolar macrophages with pHrodo™ Green *E. coli* BioParticles™ were compared between NE and IN periods. The figures (circles) of the same individual were shown connected by lines. (**D**) Correlation between the expression percentages of MHC class II and R2 (lymphocytes). Trend lines of the linear regression (solid line) and 95% confidence bands (dotted lines) analysis are shown.

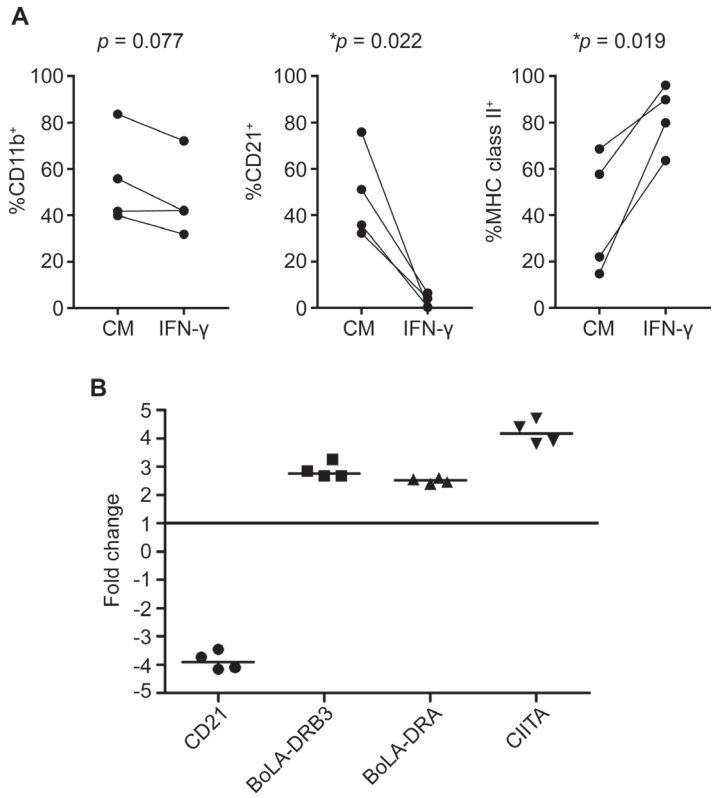

Fig. 4. (**A**) The results of CD11b, CD21, and MHC class II expression analyses in alveolar macrophages cultured in the culture medium (CM) or 5 ng/ml bovine recombinant interferon gamma (IFN-γ) for 72 hr. The circles of the same individual are connected by lines. (**B**) The changes in CD21, BoLA-DRB3, BoLA-DRA, and CIITA mRNA expression levels by IFN-γ stimulation. Analysis of relative gene expression data using real-time quantitative reverse transcription polymerase chain reaction (RT q-PCR) and the ΔΔC (T) method. Each value was normalized to that of GAPDH mRNA and fold changes of IFN-γ stimulation were calculated by referring to the value of complete medium culture. Dot plots of individual CD21 (circles), BoLA-DRB3 (square), BoLA-DRA (triangle), CIITA (inverted triangle), and mean values (horizontal bars) are shown. Data are representative of two independent experiments. The log 2-fold change values are plotted on the y-axis.

In the NE, almost all the immune cells in BALF were alveolar macrophages. In the IN, increased proportions of lymphocytes and neutrophils were observed in individuals, and there were large individual differences. Many reports have shown that in humans and experimental animals, the immune cells present in the alveolar space at a steady state are alveolar macrophages, and inflammatory cytokines, such as IFN-γ, TNF-α, and IL-1β, that are produced in response to infection or injury enhance chemokine secretion and recruit neutrophils and lymphocytes [2, 13]. It has also been reported that during the first three weeks after bronchoalveolar lavage, there is an influx of neutrophils into the lungs and changes occur in lung surfactants [22]. The present study confirmed that, in calves, the immune cells present in the alveolar space under steady state conditions are alveolar macrophages, and that some stimulation causes a change in dynamics in which lymphocytes and neutrophils infiltrate.

Although we were able to confirm the constant expression of phenotypic markers in alveolar macrophages by histogram and MFI analysis, it was difficult to calculate the percentage of expressing cells by general histogram analysis because of strong autofluorescence. Therefore, referring to the report on human alveolar macrophages [24], we were able to calculate the percentage of expressing cells by expanding the plot with strong autofluorescence and arranging the cells on the diagonal, and gating them diagonally. Based on each result, we considered the low expression of CD14 and the expression variations of CD21 and MHC Class II to be very interesting.

CD14 is one of the well-known lipopolysaccharide (LPS) receptors and is highly expressed on macrophages and monocytes [17]. Previous studies on bovine BALF have used CD14 expression to define alveolar macrophages and assess functional maturation [4, 6]. However, human and experimental animal studies have shown that phenotypic markers of alveolar macrophages are very different from those of monocytes and other macrophages, and the expression of CD14 is known to be low as in our present report [5, 19]. The expression of CD14 in bovine alveolar macrophages may be altered by infection and growth, and further studies are needed.

In addition to CD14, other surface antigens expressed by macrophages include CD172a, a membrane protein involved in phagocytosis, CD11b, CD11c, and CD21, which are complement receptors, and MHC class II, which is involved in antigen presentation. In the present study, CD21 and MHC class II were found to be expressed on alveolar macrophages and were altered by various changes in the alveolar leukocyte population. The MFI results show that CD21 expression level increased from NE to IN. At the same time, the phagocytic ability was also increased, there may be some relationship between CD21 expression and

phagocytosis, but further studies are required to elucidate its detailed function. On the other hand, the percentage of CD21-negative cells was increased in the dynamics of infiltrating neutrophils and lymphocytes. There are no reports on CD21 expression in macrophages from other tissues in cattle, which may indicate that bovine alveolar macrophages are also unique macrophages. In addition, CD21 is not expressed in human or experimental animal alveolar macrophages, even at the gene expression level [5, 19], and hence, it may be unique to cattle.

The percentage of MHC class II-positive cells was increased in proportion to the number of lymphocytes. In mice, MHC class II is expressed at low levels in the steady state, but its expression is enhanced in models of direct lung injury, such as by LPS stimulation, and enhances lung inflammation through innate and adaptive immune responses [9]. Since the expression of MHC class II on the cell surface directly indicates the strength of antigen presentation and the primary acquired immune response [15], the increase in MHC class II-positive alveolar macrophages may reflect the dynamics of the acquired immune response elicited in the bovine respiratory mucosa.

We performed *in vitro* stimulation assays to confirm whether the original alveolar macrophages were altered or whether a different cell population was introduced. Overall, IFN-γ stimulation was found to drastically decrease the expression of CD21 and increased that of MHC class II at the gene expression levels. These results suggest that bovine alveolar macrophages exhibit plasticity and function by changing their surface antigens according to the local immune dynamics of the respiratory tract. Upregulation of MHC class II by IFN-γ stimulation is well known in macrophages of various species [18], but to the best of our knowledge, the effect on CD21 expression has not been reported, and its significance will require further investigation.

The current study has some limitations. Our intention was to identify changes in immune dynamisms in respiratory mucosa of calves, particularly in alveolar macrophage properties, and to investigate convenient and simple methods for analyzing these changes. Detailed subpopulation and functional analysis as well as cell sorters and high-performance multicolor flow cytometers with multiple lasers will be required to perform accurate differential cell counts. Since this study was conducted only on calves (15–60-days old), a further study is needed to determine whether the present method can be directly applied to adult cattle and other breeds. A report suggests that the maturation of bovine alveolar macrophages is not completed until the age of 6 months [6], and hence, a longer-term study will be necessary.

In the present study, we established a convenient and high-throughput flow cytometric method for the analysis of immune cells in BALF of calves. This analysis approach can be applied to explore the pathogenesis of BRD and support vaccine research; thus, it is expected to be of great benefit to future BRD research. Using this method, we were able to shed light on the basic respiratory mucosal immune dynamics in calves and observe events in which leukocyte populations and alveolar macrophage function were drastically altered as microenvironment adaptation responses. *In vitro* analysis has shown that the function of bovine alveolar macrophages is regulated by cytokine stimulation of their own gene levels. Hence, we believe that further study of their plastic response capacity will be the key to unlocking more details about the bovine respiratory mucosal immunity. Furthermore, CD21 expression was found to be altered at the gene expression level, a characteristic unique to bovine alveolar macrophages and that suggests that human and experimental animal data cannot be directly extrapolated to studies of bovine respiratory mucosa, and that bovine respiratory mucosal immunity must be studied in cattle. In addition, our findings highlight that cattle might be an interesting subject for comparative immunological studies.

POTENTIAL CONFLICT OF INTEREST. The authors declare no conflicts of interest.

ACKNOWLEDGMENTS. This work was supported by JSPS KAKENHI Grant Number JP19K16002.

REFERENCES

1. Adair, B. M., Bradford, H. E., McNulty, M. S. and Foster, J. C. 1999. Cytotoxic interactions between bovine parainfluenza type 3 virus and bovine alveolar macrophages. *Vet. Immunol. Immunopathol.* **67**: 285–294. [Medline] [CrossRef]
2. Aggarwal, N. R., King, L. S. and D'Alessio, F. R. 2014. Diverse macrophage populations mediate acute lung inflammation and resolution. *Am. J. Physiol. Lung Cell. Mol. Physiol.* **306**: L709–L725. [Medline] [CrossRef]
3. Aulik, N. A., Hellenbrand, K. M. and Czuprynski, C. J. 2012. Mannheimia haemolytica and its leukotoxin cause macrophage extracellular trap formation by bovine macrophages. *Infect. Immun.* **80**: 1923–1933. [Medline] [CrossRef]
4. Batista, C. F., Blagitz, M. G., Santos, B. P., Bertagnon, H. G., Parra, A. C., Vianna, R. S., de Lucca, G. G., Lima, D. M., Santos, D. S. and Della Libera, A. M. 2012. Maturation of mononuclear phagocytes in the lungs of young calves-*in vitro* study. *J. Dairy Sci.* **95**: 5909–5915. [Medline] [CrossRef]
5. Berger, M., Norvell, T. M., Tosi, M. F., Emancipator, S. N., Konstan, M. W. and Schreiber, J. R. 1994. Tissue-specific Fc gamma and complement receptor expression by alveolar macrophages determines relative importance of IgG and complement in promoting phagocytosis of Pseudomonas aeruginosa. *Pediatr. Res.* **35**: 68–77. [Medline] [CrossRef]
6. Bertagnon, H. G., Batista, C. F., Santos, K. R., Gomes, R. C., Bellinazzi, J. B. and Della Libera, A. M. M. P. 2019. Alveolar macrophage functions during the transition phase to active immunity in calves. *J. Anim. Sci.* **97**: 982. [Medline] [CrossRef]
7. Brittan, M., Barr, L., Conway Morris, A., Duffin, R., Rossi, F., Johnston, S., Monro, G., Anderson, N., Rossi, A. G., McAuley, D. F., Haslett, C., Hirani, N., Dhaliwal, K. and Simpson, A. J. 2012. A novel subpopulation of monocyte-like cells in the human lung after lipopolysaccharide inhalation. *Eur. Respir. J.* **40**: 206–214. [Medline] [CrossRef]
8. Cortese, V. S. 2009. Neonatal immunology. *Vet. Clin. North Am. Food Anim. Pract.* **25**: 221–227. [Medline] [CrossRef]
9. D'Alessio, F. R., Tsushima, K., Aggarwal, N. R., Mock, J. R., Eto, Y., Garibaldi, B. T., Files, D. C., Avalos, C. R., Rodriguez, J. V., Waickman, A. T., Reddy, S. P., Pearse, D. B., Sidhaye, V. K., Hassoun, P. M., Crow, M. T. and King, L. S. 2012. Resolution of experimental lung injury by

monocyte-derived inducible nitric oxide synthase. *J. Immunol.* **189**: 2234–2245. [Medline] [CrossRef]
10. Freeman, C. M., Crudgington, S., Stolberg, V. R., Brown, J. P., Sonstein, J., Alexis, N. E., Doerschuk, C. M., Basta, P. V., Carretta, E. E., Couper, D. J., Hastie, A. T., Kaner, R. J., O'Neal, W. K., Paine, R. 3rd., Rennard, S. I., Shimbo, D., Woodruff, P. G., Zeidler, M. and Curtis, J. L. 2015. Design of a multi-center immunophenotyping analysis of peripheral blood, sputum and bronchoalveolar lavage fluid in the Subpopulations and Intermediate Outcome Measures in COPD Study (SPIROMICS). *J. Transl. Med.* **13**: 19. [Medline] [CrossRef]
11. Grant, R. A., Morales-Nebreda, L., Markov, N. S., Swaminathan, S., Querrey, M., Guzman, E. R., Abbott, D. A., Donnelly, H. K., Donayre, A., Goldberg, I. A., Klug, Z. M., Borkowski, N., Lu, Z., Kihshen, H., Politanska, Y., Sichizya, L., Kang, M., Shilatifard, A., Qi, C., Lomasney, J. W., Argento, A. C., Kruser, J. M., Malsin, E. S., Pickens, C. O., Smith, S. B., Walter, J. M., Pawlowski, A. E., Schneider, D., Nannapaneni, P., Abdala-Valencia, H., Bharat, A., Gottardi, C. J., Budinger, G. R. S., Misharin, A. V., Singer, B. D., Wunderink, R. G., Investigators N. S. S., NU SCRIPT Study Investigators. 2021. Circuits between infected macrophages and T cells in SARS-CoV-2 pneumonia. *Nature* **590**: 635–641. [Medline] [CrossRef]
12. Griffin, D., Chengappa, M. M., Kuszak, J. and McVey, D. S. 2010. Bacterial pathogens of the bovine respiratory disease complex. *Vet. Clin. North Am. Food Anim. Pract.* **26**: 381–394. [Medline] [CrossRef]
13. Herold, S., Mayer, K. and Lohmeyer, J. 2011. Acute lung injury: how macrophages orchestrate resolution of inflammation and tissue repair. *Front. Immunol.* **2**: 65. [Medline] [CrossRef]
14. Hussell, T. and Bell, T. J. 2014. Alveolar macrophages: plasticity in a tissue-specific context. *Nat. Rev. Immunol.* **14**: 81–93. [Medline] [CrossRef]
15. Inaba, K., Turley, S., Iyoda, T., Yamaide, F., Shimoyama, S., Reis e Sousa, C., Germain, R. N., Mellman, I. and Steinman, R. M. 2000. The formation of immunogenic major histocompatibility complex class II-peptide ligands in lysosomal compartments of dendritic cells is regulated by inflammatory stimuli. *J. Exp. Med.* **191**: 927–936. [Medline] [CrossRef]
16. Johnson, K. K. and Pendell, D. L. 2017. Market impacts of reducing the prevalence of bovine respiratory disease in United States beef cattle feedlots. *Front. Vet. Sci.* **4**: 189. [Medline] [CrossRef]
17. Kitchens, R. L. 2000. Role of CD14 in cellular recognition of bacterial lipopolysaccharides. *Chem. Immunol.* **74**: 61–82. [Medline] [CrossRef]
18. Mach, B., Steimle, V., Martinez-Soria, E. and Reith, W. 1996. Regulation of MHC class II genes: lessons from a disease. *Annu. Rev. Immunol.* **14**: 301–331. [Medline] [CrossRef]
19. Martin, B. K. and Weis, J. H. 1993. Murine macrophages lack expression of the Cr2-145 (CR2) and Cr2-190 (CR1) gene products. *Eur. J. Immunol.* **23**: 3037–3042. [Medline] [CrossRef]
20. Monsel, A., Lécart, S., Roquilly, A., Broquet, A., Jacqueline, C., Mirault, T., Troude, T., Fontaine-Aupart, M. P. and Asehnoune, K. 2014. Analysis of autofluorescence in polymorphonuclear neutrophils: a new tool for early infection diagnosis. *PLoS One* **9**: e92564 [CrossRef]. [Medline]
21. Perez-Casal, J., Prysliak, T., Maina, T., Suleman, M. and Jimbo, S. 2017. Status of the development of a vaccine against Mycoplasma bovis. *Vaccine* **35**: 2902–2907. [Medline] [CrossRef]
22. Reinhold, P., Becher, G. and Rothe, M. 2000. Evaluation of the measurement of leukotriene B4 concentrations in exhaled condensate as a noninvasive method for assessing mediators of inflammation in the lungs of calves. *Am. J. Vet. Res.* **61**: 742–749. [Medline] [CrossRef]
23. Soethout, E. C., Müller, K. E., van den Belt, A. J. and Rutten, V. P. 2004. Identification and phenotyping of leukocytes in bovine bronchoalveolar lavage fluid. *Clin. Diagn. Lab. Immunol.* **11**: 795–798. [Medline]
24. Weyde, J., Wassermann, K. and Schell-Frederick, E. 1997. Analysis of single and double-stained alveolar macrophages by flow cytometry. *J. Immunol. Methods* **207**: 115–123. [Medline] [CrossRef]
25. Yu, Y. R., Hotten, D. F., Malakhau, Y., Volker, E., Ghio, A. J., Noble, P. W., Kraft, M., Hollingsworth, J. W., Gunn, M. D. and Tighe, R. M. 2016. Flow cytometric analysis of myeloid cells in human blood, bronchoalveolar lavage, and Lung Tissues. *Am. J. Respir. Cell Mol. Biol.* **54**: 13–24. [Medline] [CrossRef]